Article

Thermocapillarity Motion of a Droplet within a Permeable Cavity

M.S. Faltas [1, *], H.H. Sherief [1], Alaa A. Yousef [1]

[1]*Department of Mathematics and Computer, Faculty of Science, Alexandria University, Alexandria, 21568, Egypt.*

[*] *Correspondence Address:*

M.S. Faltas: Department of Mathematics and Computer, Faculty of Science, Alexandria University, Alexandria, 21568, Egypt, E.mail address: msfaltas@sci.alex.edu.eg.

ABSTRACT: The thermocapillarity motion of a non-deformable spherical droplet embedded in a concentric permeable spherical cavity, filled with a Newtonian viscous fluid, and subjected to a uniformly prescribed temperature gradient, is investigated analytically. The energy and momentum field equations are resolved within the quasi-steady limit, considering small Péclet and Reynolds numbers. Additionally, in this investigation, it is assumed that the capillary number at the droplet interface is small, ensuring the perpetuation of the droplet's spherical shape throughout its motion. We have derived normalized thermocapillarity velocity results across a broad spectrum of relative thermal conductivity values, cavity permeabilities, and viscosity ratios. The obtained normalized thermocapillarity velocity is emphasized using graphs and tables, allowing for a comparison with existing literature data. Additionally, specific cases available in the literature have been examined to further validate our findings. This research is motivated by a variety of flow conditions, such as particle deposition in dialysis and reverse osmosis, as well as in different biological organs where fluid passes through cell cavity walls or membranes.

1. INTRODCTION

A droplet is characterized as a liquid mass surrounded by a second liquid or gaseous medium, and a bubble is identified as a gas mass within an external medium. Together, the two objects are called fluid particles. The particle's external phase is referred to as the continuous phase, and its internal phase is called the scattered phase.

When a continuous phase is mixed with a tiny droplet of the scattered phase with a temperature gradient, it exhibits motion towards the warmer region. This movement is attributed to the temperature-induced interfacial tension gradient along the droplet's surface and is recognized as thermocapillary motion [1,2]. The thermocapillary migration of liquid droplets, initially showcased through experimentation and subsequently analysed mathematically by Young et al. [3], holds significant importance in numerous practical applications [4,5]. Young et al. [3] also derived an equation for the thermocapillary velocity U_0 of a droplet with radius a immersed in an infinite Newtonian fluid of viscosity μ, when there is a constant temperature gradient $E_\infty > 0$ in the direction of $z-$axis:

$$\vec{U}_0 = -\frac{1}{(2+3\eta)(1+\frac{1}{2}k)} \frac{a\gamma_T}{\mu} \vec{E}_\infty. \qquad (1.1)$$

In this equation, k and η represent the ratios of thermal conductivities and viscosities, respectively, between the internal and ambient fluids. Additionally, $(-\gamma_T)$ denotes the variation of the interfacial tension γ at the droplet surface concerning the local temperature T. It is noteworthy to mention that equation (1.1) was independently derived by Fedosov [4]. In the majority of thermocapillary systems, as the temperature increases, the interfacial tension lowers, indicating that droplets move toward regions with higher temperatures [5]. It is important to highlight that expression (1.1) was developed under the condition of neglecting the effects of inertia and convection energy terms and assuming a small capillary number to retain the droplet's spherical shape. When the spherical droplet is sufficiently small, these hypotheses are accepted. References demonstrate how common it is in the literature to ignore the convection energy factor in the thermocapillary theory [5–14]. A spherical gas bubble's thermocapillary mobility, with its low viscosity and heat conductivity in relation to the surrounding liquid, can be determined using equation. (1.1) with the limiting values $k = 0$ and $\eta = 0$.

34

As per this equation, bubbles with a radius of 10 μm in water will undergo thermocapillary migration at a velocity of approximately 0.7 mm/s in temperature gradients of the order of 1 K/mm [2].

In many real instances of thermocapillary motion, fluid droplets are not isolated, and it is crucial to comprehend how the proximity of a boundary impacts the applicability of equation (1.1) to a fluid droplet. Quasi-steady problems related to the thermocapillary migration of a spherical gas bubble or liquid drop in the presence of boundaries have been addressed under various physical conditions and employing different methodologies e.g. [15,16]. These investigations suggest that the migration velocity of the confined drop, in comparison to that of an isolated one, diminishes as it approaches the boundary. Generally, it increases with rising values of k and η, owing to the thermal and hydrodynamic interactions between the boundary and the droplet. Chen et al. [17] addressed the thermocapillary motion of a fluid sphere moving along the central axis of an insulated circular tube, employing the boundary collocation technique for drop-to-tube radius ratios up to 0.9. They observed that the normalized migration velocity of the confined droplet consistently decreases with an increase in the radius ratio. Moreover, it was noted to increase with a decrease in k but decrease as η increases. Mahesri et al. [18] explored the impact of interface deformability on the axisymmetric thermocapillary migration of a fluid drop (with a finite capillary number) within an insulated circular tube, utilizing the boundary integral method. They found that the normalized droplet velocity exhibits an opposite trend to the results of Chen et al. [17], aligning with the outcomes of migration parallel to one or two plane walls [19]. Specifically, the normalized droplet velocity increases with an increase in η or a decrease in k, and it decreases monotonically with an increase in the drop-to-tube radius ratio.

The literature encompasses numerous studies focusing on particle interactions with naturally permeable boundaries. Examples include filter beds in water purification plants, particle deposition in reverse osmosis processes, and fluid passage through cell walls in dialysis or various biological organs. O'Neill and Bhatt [20] achieved precise Solutions to the motion of a spherical particle within a Newtonian fluid confined by a naturally permeable planar surface, utilizing bispherical coordinate.

In this study, our objective is to derive precise analytical solutions for the quasi-steady problem related to the thermocapillary migration of a droplet within a permeable spherical cavity. The impermeable cavity wall can either be insulated or specified with a linear far-field temperature distribution. A key focus of this research is to assess the influence of the permeability parameter, which characterizes the permeability of the cavity, on the thermocapillary velocity.

2. Equations Governing Thermal Transport and Momentum

The equations that describe the flow of an incompressible Newtonian fluid without external body forces are [21]:

$$\nabla \cdot \vec{u} = 0, \tag{2.1}$$

$$\rho \left(\frac{\partial \vec{u}}{\partial t} + \vec{u} \cdot \nabla \vec{u} \right) = -\nabla p - \mu \nabla \wedge \nabla \wedge \vec{u}, \tag{2.2}$$

and the equation that describes the thermal transport in a fluid is

$$\frac{\partial T}{\partial t} + \vec{u} \cdot \nabla T = \frac{k}{\rho c_p} \nabla^2 T. \tag{2.3}$$

Here, $\vec{u}$, T, and p represent the velocity, pressure, and temperature, respectively. The constants $\left(\rho, \mu, k, c_p \right)$ correspond to the density, viscosity coefficient, thermal conductivity, and specific heat. The constitutive equations governing the flow are as follow:

$$\Pi = -pI + \mu \left(\nabla \vec{u} + \nabla^T \vec{u} \right), \tag{2.4}$$

$$\vec{q} = -k \nabla T, \tag{2.5}$$

Here, Π is the stress tensor, $\vec{q}$ is the heat flux vector, I is a unit dyadic, and $(.)^T$ denotes the transpose of a dyadic.

3. Description of the Problem

Consider the quasisteady axially symmetric thermophoresis movement of a sphere droplet. Of radius a, viscosity μ_d and thermal conductivity k_d situated instantaneously at the center of a naturally permeable cavity of radius b filled with a Newtonian viscous fluid of viscosity μ and thermal conductivity k_f. The region outside the cavity is filled with a porous medium of small permeability K. The particle translates along a vertical diameter with a velocity U, as shown in **Figure. 1.** Consider (r, θ, ϕ) as a set of spherical coordinates centred at the origin and let $\left(\vec{e}_r, \vec{e}_\theta, \vec{e}_\phi \right)$ represent the corresponding unit vectors. In the porous region outside the cavity, a constant temperature gradient $\vec{E}_\infty = E_\infty \vec{e}_z \left(E_\infty > 0 \right)$ ($\vec{e}_z$ is a unit vector in the direction of $z-$axis) is applied parallel to a vertical diameter. It is assumed that all thermal properties of the system remain constants.
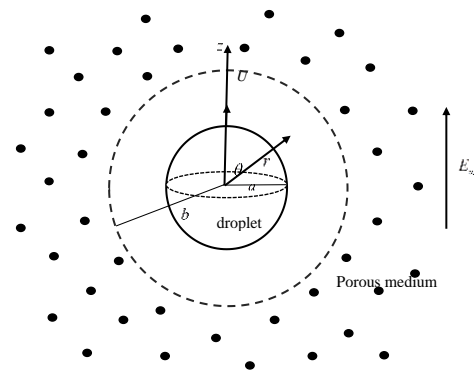

Figure 1. Geometrical sketch of a thermocapillarity droplet translates within permeable cavity.

The objective of this study is to investigate how the permeable cavity wall influence droplet mobility. To determine the droplet's thermocapillarity velocity, Determining the temperature both within and outside the droplet is crucial at first, as well as the fluid velocity distributions in both regions.

In instances where the temperature varies with time at any position within the system, the heat transfer is characterized as transient or unsteady state. Many practical scenarios involving heat transfer under different physical conditions, a steady-state temperature is established once the transient period concludes. If external temperature changes or internal heat generation occurs too rapidly to reach a steady state, the system remains in a state of continual change. Consequently, It makes sense to take into account a steady-state temperature for the cavity's fluid as well as the droplet. Additionally, When there is little droplet size and slow fluid flow, the Reynolds and Péclet numbers are significantly low. In these cases, convective effects are disregarded and heat energy transfer between the fluid and droplet mostly happens through heat conduction [22]. Nevertheless, for larger droplet undergoing thermocapillarity in high-temperature gradients, the Péclet number values could be around 0.1, and It is impossible to ignore convective heat transfer when compared to fluid conduction [23]. Hence, assuming steady-state conditions and low Reynolds and Péclet numbers, equations (2.2) and (2.3) can be simplified to:

$$\left. \begin{array}{l} \nabla p - \mu_f \nabla^2 \vec{u} = 0, \quad a \le r \le b \\ \nabla p_d - \mu_d \nabla^2 \vec{u}_d = 0, \quad r \le a \end{array} \right\} \tag{3.1}$$

$$\left. \begin{array}{l} \nabla^2 T = 0, \quad a \le r \le b \\ \nabla^2 T_d = 0. \quad r \le a \end{array} \right\} \tag{3.2}$$

4. Permeability of the Cavity Wall

To grasp the interaction between the droplet and the permeable cavity wall, it is crucial to consider the outer surrounding region of the cavity wall $r \ge b$ as a porous material. This porous region is represented in our model using Darcy's law:

$$\nabla P = -\frac{\mu}{K} \vec{v}, \quad r \ge b \tag{4.1}$$

In this context, ∇P represents the pressure gradient within the porous medium $r \ge b$, and $\vec{v}$ denotes the filter velocity. The permeability coefficient K remains unaffected by the fluid's nature but is contingent upon the medium's geometry. The next step involves determining the appropriate boundary condition for the naturally permeable cavity wall. Beavers and Joseph [24] conducted experimental studies revealing the inaccuracy of the no-slip condition at naturally permeable walls. Instead, they proposed the following semiempirical slip condition:

$$\frac{\partial u_s}{\partial n} = -\frac{\beta}{\sqrt{K}} (u_s - v_s), \tag{4.2}$$

where n and s representing distances normal and tangential to the permeable cavity wall, respectively, and β indicating a nondimensional slip parameter dependent on the porous medium's structure. Saffman [25] provided a theoretical justification for Equation (4.1) when dealing with small permeability values K. This reasoning required balancing flows in the Stokes and Darcy regions using a boundary layer. Additionally, Saffman demonstrated that for small permeability

values, $\vec{v} = O(K)$, allowing $\vec{v}$ to be considered zero $(\vec{v} = 0)$. Consequently, for low permeability values K, the Stokes region flow's first-order solution is still applicable,

$$u_s = \frac{\sqrt{K}}{\beta} \frac{\partial u_s}{\partial n}, \tag{4.3}$$

at the naturally permeable cavity wall, Condition (4.3) has been used by many authors, for example, [16, 20].

5. Distribution of Thermal Transport

In order to determine solutions for equations (3.2), which govern the temperatures T and the boundary conditions at the droplet's surface and the permeable cavity wall must be specified. The usual heat flux and temperature continuity at the droplet surface are determined by the boundary conditions. Additionally, they specify that the local temperature gradient at the cavity wall should align parallel to the uniformly applied temperature gradient in the absence of the droplet. Thus,

$$\left. \begin{array}{l} T = T_d, \\ k_f \frac{\partial T}{\partial r} = k_d \frac{\partial T_d}{\partial r}, r = a \end{array} \right\} \tag{5.1}$$

The boundary condition at the permeable cavity is given by,

$$\frac{\partial T}{\partial r} = E_\infty \cos\theta, \quad r = b \tag{5.2}$$

The boundary condition for the temperature at the cavity surface can be considered as the distribution that induces the gradient $E_\infty \vec{e}_z$ in the system in the absence of the droplet. In this scenario, Equation (5.2) transforms into

$$T = T_0 + E_\infty r \cos\theta, \quad r = b \tag{5.3}$$

where T_0 is the temperature at the center of the droplet. These conditions should be supplemented with the boundedness condition of T_d as $r \to 0$.

The solutions of (3.2) and (5.1) - (5.3) are [26],

$$T_d = T_0 + 3\delta E_\infty r \cos\theta \quad (r \le a), \tag{5.4}$$

$$T = T_0 + \delta\left(1 - k + (k+2)a^3 r^{-3}\right) E_\infty r \cos\theta \quad (a \le r \le b), \tag{5.5}$$

$k = k_d / k_f$ represents the ratio between the thermal conductivities of the droplet and the fluid within the cavity. Here, when the boundary condition (5.2) is used, δ is given by,

$$\delta = \left(k + 2 - 2(1-k)\sigma^3\right)^{-1}, \tag{5.6}$$

while when the boundary condition (5.3) is used we obtain δ as

$$\delta = \left(k + 2 + (1-k)\sigma^3\right)^{-1}, \tag{5.7}$$

where $\sigma = a / b$ is the ratio of the between the radii of the droplet and cavity.

6. Distribution of Components of Velocity

Having obtained information about the temperature distribution solution, we can now move forward to determine the flow field within the droplet and cavity. The assumption is made that the fluids exhibit Newtonian behavior and are incompressible both inside and outside the droplet. Owing to the low Reynolds

number, a quasisteady fourth-order differential equation characterizing viscous axisymmetric flow governs the fluid motion caused by the droplet's thermocapillarity migration.

Since fluid motion is axisymmetric, the velocity components of the fluids can be depicted in terms of the Stokes stream functions ψ, $(a \leq r \leq b)$ and ψ_d, $(r \leq a)$ through the relations,

$$u_r = -\frac{1}{r^2 \sin \theta} \frac{\partial \psi}{\partial \theta}, \quad u_\theta = \frac{1}{r \sin \theta} \frac{\partial \psi}{\partial r}, \tag{6.1}$$

$$u_{rd} = -\frac{1}{r^2 \sin \theta} \frac{\partial \psi_d}{\partial \theta}, \quad u_{\theta d} = \frac{1}{r \sin \theta} \frac{\partial \psi_d}{\partial r} \tag{6.2}$$

Inserting (6.1) and (6.2) into (3.1), we obtain the differential equations satisfied by the stream functions as

$$E^4 \psi = 0, \qquad (a \leq r \leq b) \tag{6.3}$$

$$E^4 \psi_d = 0, \qquad (r \leq a) \tag{6.4}$$

where $E^2 = \frac{\partial^2}{\partial r^2} + \frac{\sin \theta}{r^2} \frac{\partial}{\partial \theta} \frac{1}{r \sin \theta} \frac{\partial}{\partial \theta}$ is the Stokes operator.

The boundary condition for the fluid velocity at the droplet surface $r = a$ are,

$$u_r = U \cos \theta, \tag{6.5}$$

$$u_{rd} = U \cos \theta, \tag{6.6}$$

$$u_\theta = u_{\theta d}, \tag{6.7}$$

$$\Pi_{r\theta} - \Pi_{r\theta d} = -\gamma_T \frac{1}{r} \frac{\partial T}{\partial \theta}. \tag{6.8}$$

Here $\vec{U} = U \, \vec{e}_z$ is the thermocapillarity migration velocity to be specified. Note that $\gamma_T \left(= \frac{\partial \gamma}{\partial T} \right)$ assumed to be constant on the scale of the droplet radius. Also note that $\frac{1}{r} \frac{\partial T}{\partial \theta}$ able can be assessed from the temperature distribution given by (5.5). The expressions of the tangential stresses $\Pi_{r\theta}$ and $\Pi_{r\theta d}$ can be found from the constitutive (2.4) as

$$\Pi_{r\theta} = \mu \left(r \frac{\partial}{\partial r} \left(\frac{q_\theta}{r} \right) + \frac{1}{r} \frac{\partial q_r}{\partial \theta} \right) \tag{6.9}$$

$$\Pi_{r\theta d} = \mu_d \left(r \frac{\partial}{\partial r} \left(\frac{q_{\theta d}}{r} \right) + \frac{1}{r} \frac{\partial q_{rd}}{\partial \theta} \right) \tag{6.10}$$

The boundary condition at the permeable cavity wall $r = b$ are,

$$u_r = 0, \tag{6.11}$$

$$\frac{\partial u_\theta}{\partial r} = -\bar{\lambda} u_\theta. \tag{6.12}$$

Where $\bar{\lambda} = \frac{\beta}{\sqrt{K}}$ is the permeability of the cavity wall slip parameter with dimension $(\text{length})^{-1}$. The limiting cases $\bar{\lambda} \to \infty$ and $\bar{\lambda} = 0$, correspond, respectively, to the rigid cavity walls and cavity with free surface. In addition to the above condition, we have

$$\lim_{r \to 0} \vec{u}_d = 0. \tag{6.13}$$

Solutions of (6.3) and (6.4) appropriate to satisfy the stated boundary conditions are given by:

$$\psi = \left(Cr^{-1} + Dr + Er^2 + Fr^4 \right) \sin^2 \theta, \tag{6.14}$$

$$\psi_d = \left(E_1 r^2 + F_1 r^4 \right) \sin^2 \theta, \tag{6.15}$$

where the unknown constants C, D, E, F, E_1 and F_1 are to be determined.

Inserting (6.14) and (6.15) into (6.1), (6.2), (6.9) and (6.10), we obtain,

$$u_r = -2 \left(Cr^{-3} + Dr^{-1} + E + Fr^2 \right) \cos \theta, \tag{6.16}$$

$$u_\theta = \left(-Cr^{-3} + Dr^{-1} + 2E + 4Fr^2 \right) \sin \theta, \tag{6.17}$$

$$\Pi_{r\theta} = 6\mu \left(Cr^{-4} + Fr \right) \sin \theta, \tag{6.18}$$

$$u_{rd} = -2 \left(E_1 + F_1 r^2 \right) \cos \theta, \tag{6.19}$$

$$u_{\theta d} = \left(2E_1 + 4F_1 r^2 \right) \sin \theta, \tag{6.20}$$

$$\Pi_{r\theta d} = 6\mu_d F_1 r \sin \theta. \tag{6.21}$$

We obtain also,

$$\frac{1}{r} \frac{\partial T}{\partial \theta} = -\delta \left(1 - k + (k+2) a^3 r^{-3} \right) E_\infty \sin \theta. \tag{6.22}$$

Applying the boundary conditions by inserting (6.16) - (6.22) into (6.5) - (6.8), (6.11) and (6.12), We get the following set of equations to determine the unknown constants C, D, E, F, E_1 and F_1:

$$\left. \begin{aligned}
& Ca^{-3} + Da^{-1} + E + Fa^2 = -\tfrac{1}{2} U, \\
& E_1 + F_1 a^2 = -\tfrac{1}{2} U, \\
& -Ca^{-3} + Da^{-1} + 2E + 4Fa^2 - 2E_1 - 4F_1 a^2 = 0, \\
& Ca^{-3} + Fa^2 - \eta F_1 a^2 = -\tfrac{1}{2} U_0 \delta, \\
& Ca^{-3}\sigma^3 + Da^{-1}\sigma + E + Fa^2\sigma^{-2} = 0, \\
& \sigma^3 (3\sigma - \lambda) Ca^{-3} + \sigma(\lambda - \sigma) Da^{-1} + 2\lambda E + 4\sigma^{-1}\left(2 + \lambda\sigma^{-1}\right) Fa^2 = 0,
\end{aligned} \right\} \tag{6.23}$$

Where $U_0 = -\dfrac{a\gamma_T E_\infty}{\mu}$ is a characteristic velocity, $\eta = \dfrac{\mu_d}{\mu}$ is the viscosity ratio between the droplet and the fluid within the cavity, and $\lambda = \bar{\lambda} a$ is a non-dimensional parameter representing the permeability of the cavity wall. The solution of the set of equations (6.23) is given by:

$$\left. \begin{aligned}
C = a^3 \Delta & \left[U \left(\lambda \left(-\eta + (\eta - 1)\sigma^3 \right) - 4\eta\sigma + (\eta - 1)\sigma^4 \right) \right. \\
& \left. + U_0 \delta \left(\lambda \left(2 - 3\sigma + \sigma^3 \right) + 8\sigma - 9\sigma^2 + \sigma^4 \right) \right],
\end{aligned} \right\} \tag{6.24}$$

$$\left. \begin{aligned}
D = a \Delta & \left[U \left(\lambda \left(2 + 3\eta + 3(1 - \eta)\sigma^5 \right) + 4(2 + 3\eta)\sigma + 3(\eta - 1)\sigma^6 \right) \right. \\
& \left. + U_0 \delta \left(\lambda \left(-2 + 5\sigma^3 - 3\sigma^5 \right) - 8\sigma + 5\sigma^4 + 3\sigma^6 \right) \right],
\end{aligned} \right\} \tag{6.25}$$

$$E = \tfrac{1}{2}\Delta\Big[U\big(\lambda\big(-3(2+3\eta)\sigma+5\eta\sigma^3+4(\eta-1)\sigma^6\big)-9(2+3\eta)\sigma^2+5\eta\sigma^4+8(1-\eta)\sigma^7\big) \\ +U_0\delta\big(\lambda\big(6\sigma-10\sigma^3+4\sigma^6\big)+18\sigma^2-10\sigma^4-8\sigma^7\big)\Big], \tag{6.26}$$

$$F = -\tfrac{1}{2}a^{-2}\Delta\Big[U\big(\lambda\big((-2-3\eta)\sigma^3+3\eta\sigma^5\big)-(2+3\eta)\sigma^4-3\eta\sigma^6\big) \\ +U_0\delta\big(\lambda\big(2\sigma^3-6\sigma^5+4\sigma^6\big)+2\sigma^4+6\sigma^6-8\sigma^7\big)\Big], \tag{6.27}$$

$$E_1 = \tfrac{1}{2}\Delta'\big(U\big(\lambda\sigma_5+\sigma_6\big)+U_0\delta\big(\lambda\sigma_7+\sigma_8\big)\big), \tag{6.28}$$

$$F_1 = -\tfrac{1}{2}a^{-2}\Delta'\Big[U\big(\lambda\big(2+2\sigma+2\sigma^2-3\sigma^3-3\sigma^4\big)+8\sigma+8\sigma^2+8\sigma^3+3\sigma^4+3\sigma^5\big) \\ +U_0\delta\big(\lambda\sigma_7+\sigma_8\big)\Big]. \tag{6.29}$$

Here,

$$\Delta = \big(\lambda\sigma_1+\sigma_2\big)^{-1},\ \Delta' = \big(\lambda\sigma_3+\sigma_4\big)^{-1},$$
$$\sigma_1 = -4(1+\eta)+3(2+3\eta)\sigma-10\eta\sigma^3+3(3\eta-2)\sigma^5+4(1-\eta)\sigma^6,$$
$$\sigma_2 = -16(1+\eta)\sigma+9(2+3\eta)\sigma^2-10\eta\sigma^4+3(2-3\eta)\sigma^6+8(\eta-1)\sigma^7,$$
$$\sigma_3 = -4(1+\eta)+(2+5\eta)\sigma+(2+5\eta)\sigma^2+(2-5\eta)\sigma^3+(2-5\eta)\sigma^4+4(\eta-1)\sigma^5,$$
$$\sigma_4 = -16(1+\eta)\sigma+(2+11\eta)\sigma^2+(2+11\eta)\sigma^3+(2+\eta)\sigma^4+(2+\eta)\sigma^5+8(1-\eta)\sigma^6, \tag{6.30}$$

$$\sigma_5 = 6+4\eta-5\eta\sigma-5\eta\sigma^2+5(\eta-1)\sigma^3+5(\eta-1)\sigma^4+4(1-\eta)\sigma^5,$$
$$\sigma_6 = 8(3+2\eta)\sigma+(6-11\eta)\sigma^2+(6-11\eta)\sigma^3+(1-\eta)\sigma^4+(1-\eta)\sigma^5+8(\eta-1)\sigma^6,$$
$$\sigma_7 = 4-5\sigma-5\sigma^2+5\sigma^3+5\sigma^4-4\sigma^5,$$
$$\sigma_8 = 16\sigma-11\sigma^2-11\sigma^3-\sigma^4-\sigma^5+8\sigma^6. \tag{6.31}$$

Thermocapillarity migration velocity

The external fluid exerts a drag force F_z in the $z-$ direction on the droplet, given by [21]

$$F_z = 8\pi\mu D. \tag{6.32}$$

As the droplet is in free suspension within the surrounding fluid, the resultant force from externally fluid must be zero, $D = 0$. Under this constraint, equation (6.25) provides the thermocapillarity migration velocity in the form:

$$\frac{U}{U_0} = \frac{\big(8\sigma-5\sigma^4-3\sigma^6+(2-5\sigma^3+3\sigma^5)\lambda\big)\delta}{4(2+3\eta)\sigma+3(\eta-1)\sigma^6+(2+3\eta+3(1-\eta)\sigma^5)\lambda}. \tag{6.33}$$

We record the following particular cases:

• For rigid cavity, $\lambda \to \infty$

$$\frac{U}{U_0} = \frac{\big(2-5\sigma^3+3\sigma^5\big)\delta}{2+3\eta+3(1-\eta)\sigma^5} \tag{6.34}$$

• For free surface cavity, a completely permeable cavity, $\lambda = 0$

$$\frac{U}{U_0} = \frac{\big(8-5\sigma^3-3\sigma^5\big)\delta}{4(2+3\eta)+3(\eta-1)\sigma^5}. \tag{6.35}$$

• For a gas bubble in a permeable cavity, $\eta = 0$

$$\frac{U}{U_0} = \frac{\big(8\sigma-5\sigma^4-3\sigma^6+(2-5\sigma^3+3\sigma^5)\lambda\big)\delta}{8\sigma-3\sigma^6+(2+3\sigma^5)\lambda}. \tag{6.36}$$

• For droplet in an unbounded viscous fluid $\sigma \to 0$,

$$\frac{U}{U_0} = \frac{2\delta}{2+3\eta}, \tag{6.37}$$

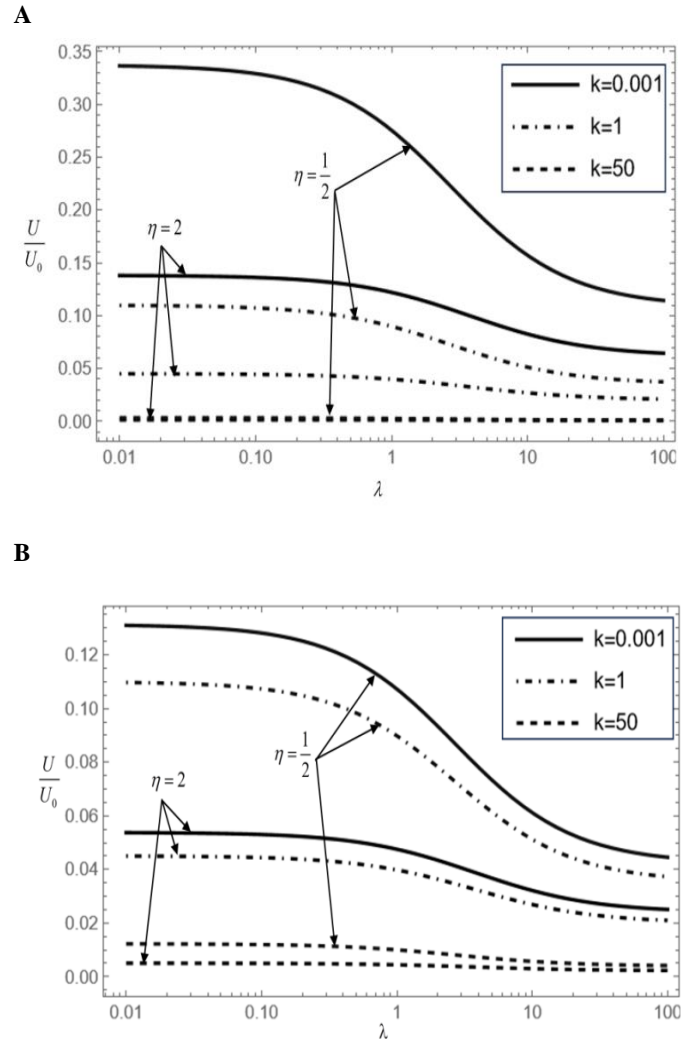with $\delta = (k+2)^{-1}$, which recovers the result (1.1).

A

B

Figure 2. Normalized thermocapillarity migration velocity versus the permeability of the cavity λ for different thermal conductivity parameter k with viscosity ratio, $\eta = 0.5$, $\eta = 2$, and $\sigma = 0.8$ (A) case I and (B) case II.
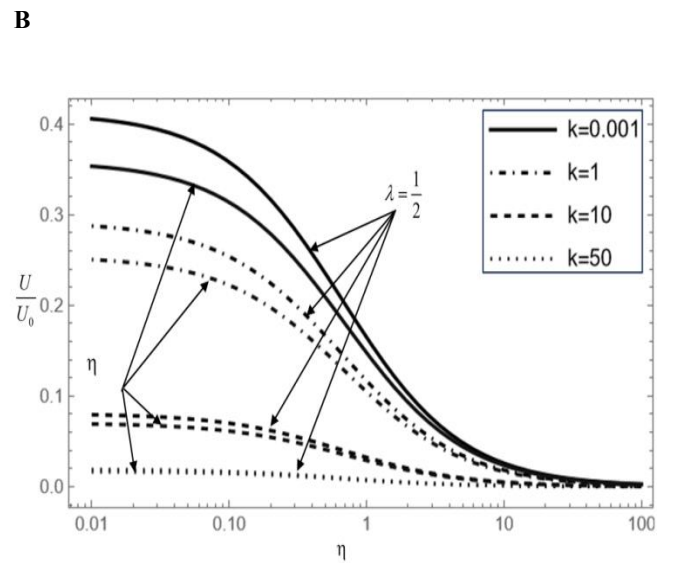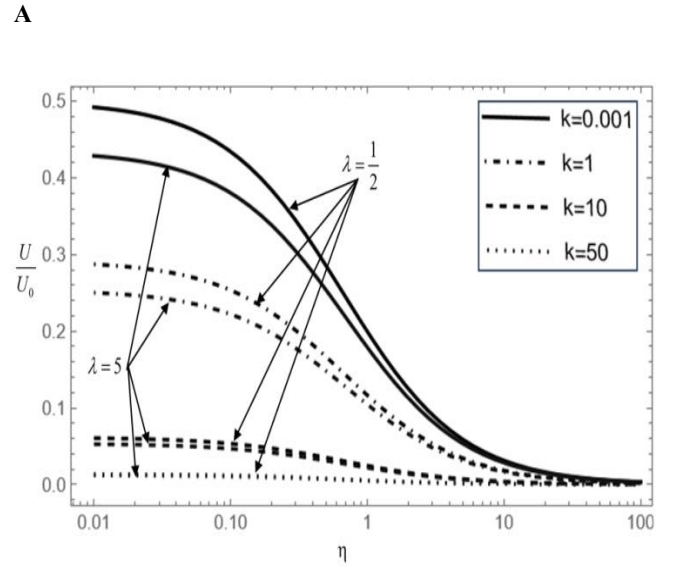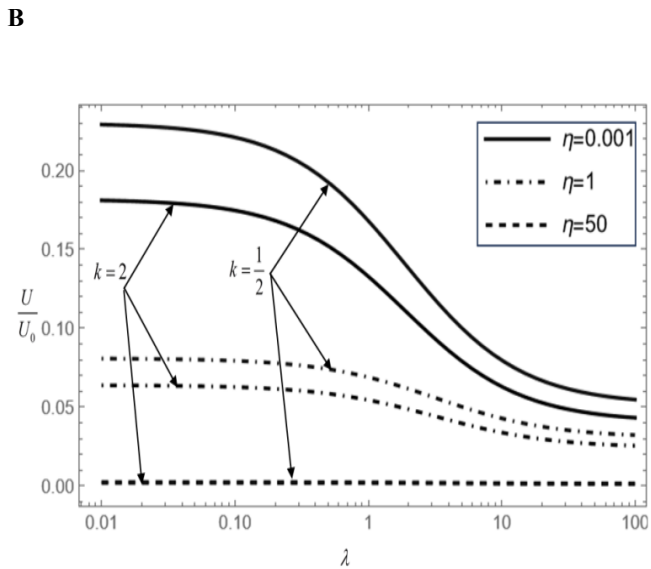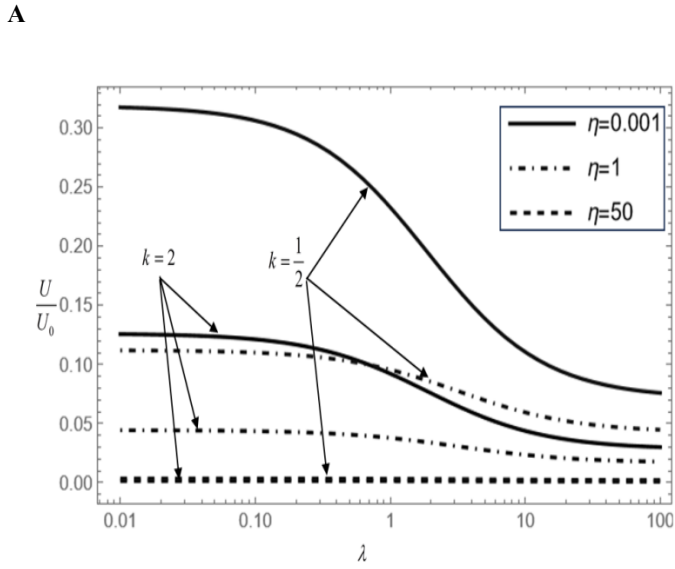
A

B

Figure 3. Normalized thermocapillarity migration velocity versus the permeability of the cavity λ for different viscosity ratio η with thermal conductivity parameter, $k = 0.5$, $k = 2$, and $\sigma = 0.8$ (A) case I and (B) case II.

A

B

Figure 4. Normalized thermocapillarity migration velocity versus the viscosity ratio η for different thermal conductivity parameter k with permeability parameter $\lambda = 0.5$, 5 and $\sigma = 0.8$ (A) case I and (B) case II.
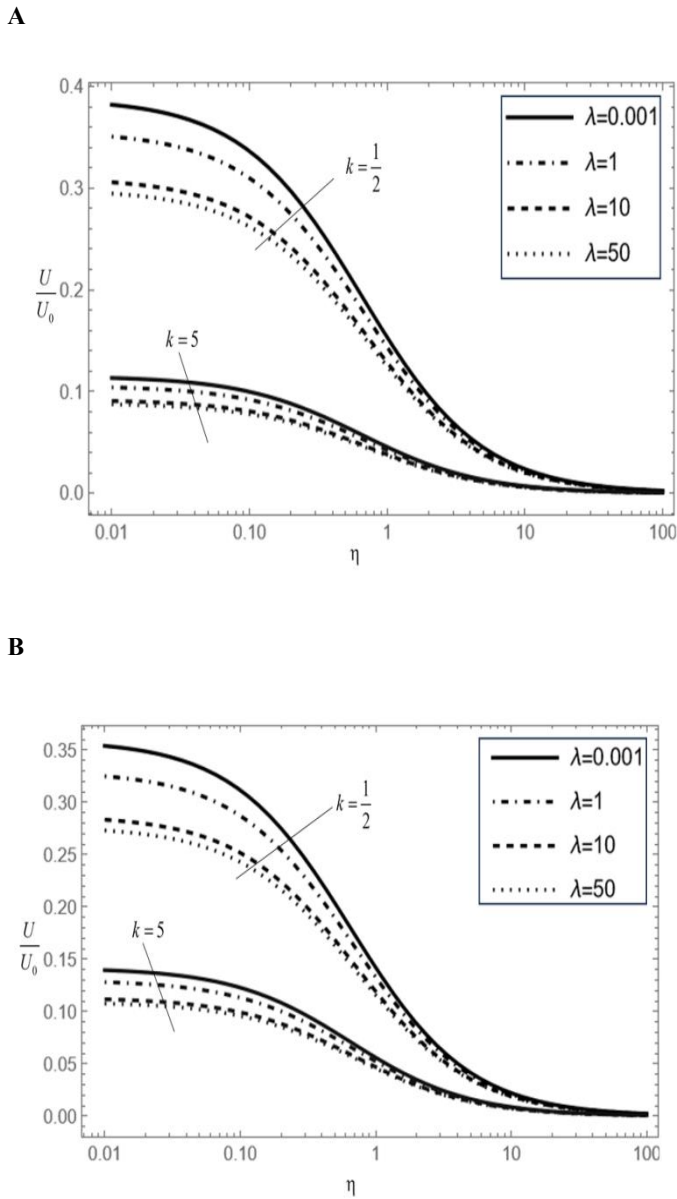
A

B

Figure 5. Normalized thermocapillarity migration velocity versus the viscosity ratio η for different permeability parameter λ with for thermal conductivity $k = 0.5,\ 5$ and $\sigma = 0.5$ (A) case I and (B) case II.
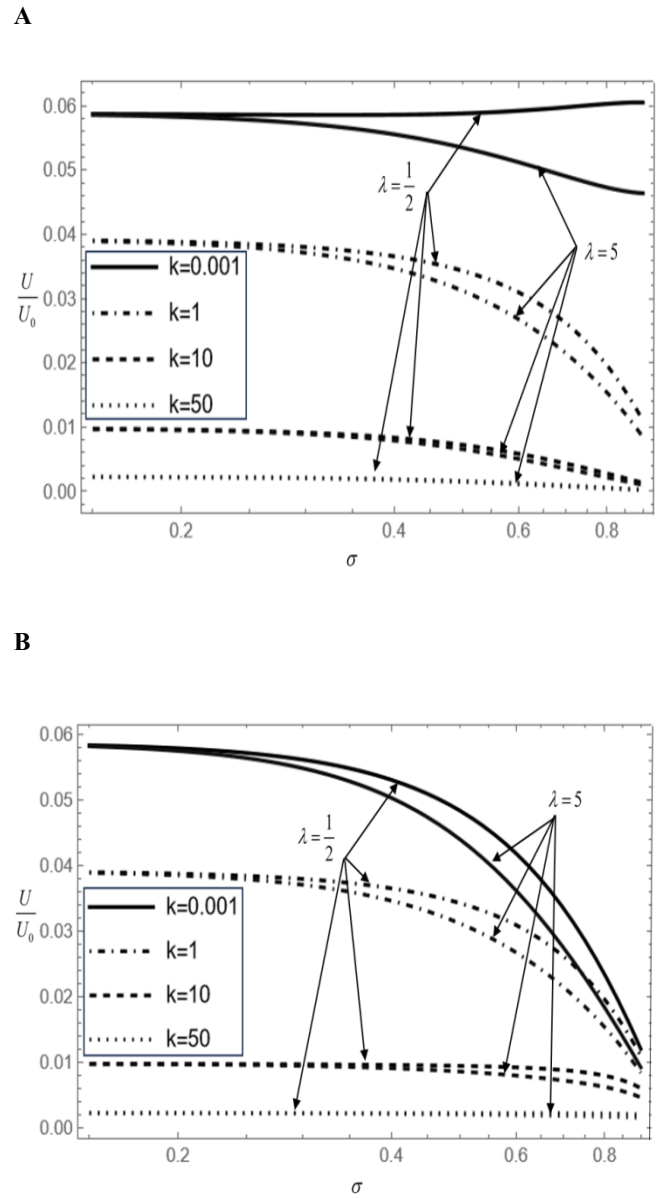
A

B

Figure 6. Normalized thermocapillarity migration velocity versus the radii ratio σ for different for thermal conductivity k with permeability $\lambda = 0.5,\ 5$ and $\eta = 5$ (A) case I and (B) case II.

40

A
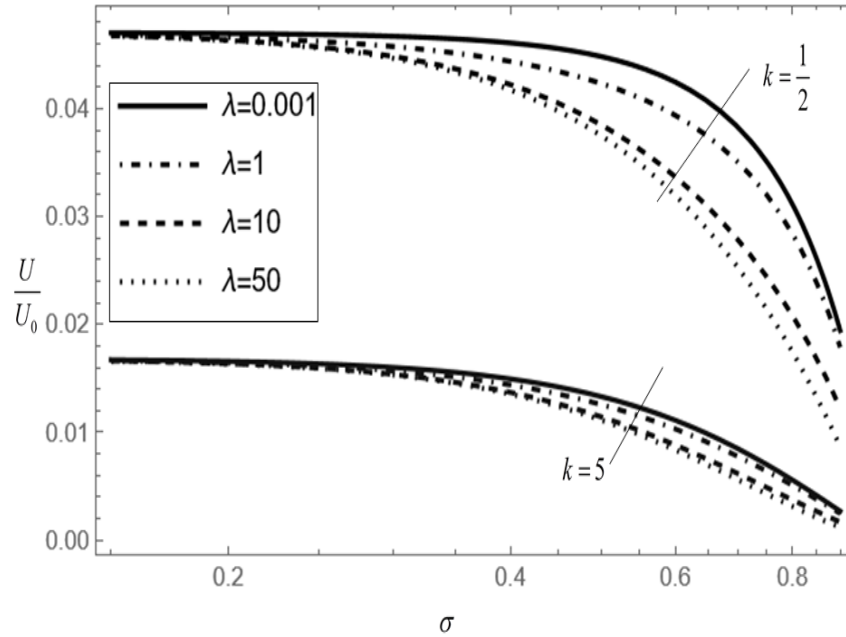
B

Figure 7. Normalized thermocapillarity migration velocity versus the radii ratio σ for different permeability λ with thermal conductivity $k = 0.5, 5$ and $\eta = 5$ (A) case I and (B) case II.
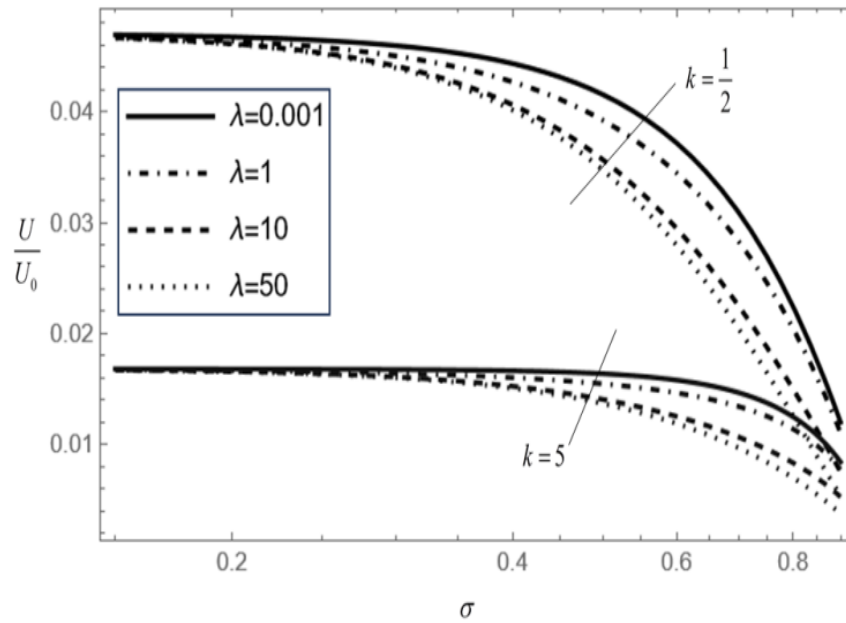
Table 1. The thermocapillarity migration velocity U/U_0 versus the permeability of the cavity λ for different viscosity ratio $\eta=0, \eta=1, \eta=100$ with $k=0$ and $\sigma=0.8$ for the case I

k = 0	σ = 0.8		
λ	η = 0	η = 1	η = 100
0	0.650789	0.228328	0.00349842
0.1	0.625283	0.224036	0.00347187
0.5	0.544675	0.209187	0.00337518
1	0.475384	0.194604	0.00327214
5	0.283527	0.141962	0.00281501
10	0.225361	0.121025	0.00258413
100	0.154639	0.0910804	0.00218469

Table 2. The thermocapillarity migration velocity U/U_0 versus the permeability of the cavity λ for different thermal conductivity $k=1, k=10$ with $\eta=5$ and $\sigma=0.5$ for the case I

η = 5	σ = 0.5	
λ	k = 1	k = 10
0	0.0354966	0.00747298
0.1	0.0352162	0.00741393
1	0.0335178	0.00705639
10	0.0304802	0.00641688
100	0.0295705	0.00622537

Table 3. The thermocapillarity migration velocity U/U_0 versus the permeability of the cavity λ for different viscosity ratio $\eta=0, \eta=1, \eta=100$ with $k=0$ and $\sigma=0.8$ for the case II

k = 0	σ = 0.8		
λ	η = 0	η = 1	η = 100
0	0.252854	0.0887134	0.00135926
0.1	0.242944	0.0870457	0.00134894
0.5	0.211626	0.0812766	0.00131138
1	0.184703	0.0756106	0.00127134
5	0.11016	0.0551574	0.00109373
10	0.0875605	0.0470226	0.00100403
100	0.0600827	0.0353879	0.000848831

Table 4. The thermocapillarity migration velocity U/U_0 versus the permeability of the cavity λ for different thermal conductivity $k=1, k=10$ with $\eta=5$ and $\sigma=0.5$ for the case II

η = 5	σ = 0.5	
λ	k = 1	k = 10
0	0.354966	0.00979218
0.1	0.0352162	0.00971481
1	0.0335178	0.0092463
10	0.0304802	0.00840833
100	0.0295705	0.00815738

7. Results and Discussions

The graphical representations of the normalized thermocapillarity migration velocity U/U_0 given by (2.6.33), are presented for various non-dimensional parameters:

1. The permeability parameter of the cavity wall λ $(0 \le \lambda < \infty)$, this parameter measures the permeability of the cavity wall. The value $\lambda = 0$ represents a perfect permeation of the cavity wall, while $\lambda \to \infty$ represents impermeable cavity wall (solid wall).

2. The viscosity ratio $\eta (= \mu_1/\mu)$, this ratio ranges from zero to infinity. The value $\eta = 0$ represents a gas bubble.

3. The thermal conductivity parameter $k (= k_1/k)$.

4. The radii parameter $\sigma (= a/b), \sigma = 0$ represents a droplet moving thermally in an unbounded viscous medium.

Because of variations in the boundary conditions of the temperature solutions on the surface of the permeable cavity, two cases can be established: Case I, the boundary condition (2.5.2) is used in which $\delta = \left(k + 2 - 2(1-k)\sigma^3\right)^{-1}$, and Case II, the boundary condition (2.5.3) is used in which $\delta = \left(k + 2 + (1-k)\sigma^3\right)^{-1}$. In the following figures, case I labelled as (A) and case II labelled as (B).

Figures. 2 and 3 represent plots for the normalized thermocapillarity migration velocity U/U_0 versus the permeability of the cavity λ. For the entire range of thermal conductivity parameter, k and viscosity ratio η, the normalised migration velocity U/U_0 decreases monotonically as the permeability parameter increases. For fixed value of permeability parameter λ, the normalized migration U/U_0 increases as the conductivity parameter k and the viscosity ratio η decrease with $U/U_0 \to 0$ as k and η increase indefinitely. It observed that the values of U/U_0 are greater for case I than the values for the case II with respect to the permeability of the cavity.

Figures. 4 and 5 represent plots for the normalized thermocapillarity migration velocity U/U_0 versus the viscosity ratio η. For the entire range of thermal conductivity parameter, k and permeability parameter λ, the normalised migration velocity U/U_0 decreases monotonically as the viscosity ratio increases. For fixed value of viscosity ratio η, the normalized migration U/U_0 increases as the conductivity parameter k and the permeability parameter λ decrease. For large values of thermal conductivity parameter $(k > 10)$, the normalized migration U/U_0 is almost has the same values for the entire range of permeability parameter λ.

It observed also that the values of U/U_0 are greater for case I than the values for the case II with respect to the viscosity ratio.

Figures. 6 and 7 represent plots for the normalized thermocapillarity migration velocity U/U_0 versus the radii ratio σ. For the entire range of thermal conductivity parameter, k and permeability parameter $\lambda > 1$, the normalised migration velocity U/U_0 decreases monotonically as the radii ratio increases. For fixed radii ratio σ, the normalized thermocapillarity migration velocity U/U_0 increases with the decrease of k and λ.

Table. 1 The thermocapillarity migration velocity U/U_0 versus the permeability of the cavity λ for different viscosity ratio $\eta = 0, \eta = 1, \eta = 100$ for the case I, the normalised migration velocity U/U_0 decreases as the permeability of the cavity λ increases. For fixed $k = 0$ and $\sigma = 0.8$.

Table. 2 The thermocapillarity migration velocity U/U_0 versus the permeability of the cavity λ for different thermal conductivity $k = 1, k = 10$ for the case I, the normalised migration velocity U/U_0 decreases as the permeability of the cavity λ increases. For fixed $\eta = 5$ and $\sigma = 0.5$.

Table. 3 The thermocapillarity migration velocity U/U_0 versus the permeability of the cavity λ for different viscosity ratio $\eta = 0, \eta = 1, \eta = 100$ for the case II, the normalised migration velocity U/U_0 decreases as the permeability of the cavity λ increases. For fixed $k = 0$ and $\sigma = 0.8$.

Table. 4 The thermocapillarity migration velocity U/U_0 versus the permeability of the cavity λ for different thermal conductivity $k = 1, k = 10$ for the case II, the normalised migration velocity U/U_0 decreases as the permeability of the cavity λ increases. For fixed $\eta = 5$ and $\sigma = 0.5$.

8. Conclusions

This article explores the theoretical analysis of the quasisteady axisymmetric thermocapillarity slow motion of a spherical droplet positioned concentrically within a spherical permeable cavity wall. The investigation focuses on the limit where the Péclet number is considered negligible. The system experiences a uniformly specified temperature gradient. In this study, In order to guarantee that the droplet keeps its spherical shape during its journey, we assume a minimal capillary number at the droplet interface. By employing the energy and momentum equations, An equation for the normalized thermocapillary migration velocity was obtained by considering pertinent geometrical and physical characteristics.

Our results are compared with the available data in the literature. The primary discovery in this research is that the normalized thermocapillary migration velocity decreases monotonically as the permeability of the cavity, viscosity ratio, thermal conductivity ratio, and radii ratio increase. This investigation draws inspiration from a range of flow scenarios, encompassing particle deposition in processes such as reverse osmosis, dialysis, and within different biological organs where fluids traverse membranes or cell cavity walls.

References

[1] Keh, H.J.; Chen, S.H. The axisymmetric thermocapillary motion of two fluid droplets, Int. J. Multiph. Flow. 1990, 16 (3), 515–527.

[2] Lee, T.C.; Keh, H.J. Axisymmetric thermocapillary migration of a fluid sphere in a spherical cavity, Int. J. Heat Mass Transfer. 2013, 62, 772–781.

[3] Young, N.O.; Goldstein, J.S.; Block, M. J. The motion of bubbles in a vertical temperature gradient, J. Fluid Mech. 1959, 6(3), 350–356.

[4] Selva, B.; Cantat, I.; Jullien, M.-C. Temperature-induced migration of a bubble in a soft microcavity, Physics of Fluids. 2011, 23(5), 052002.

[5] Subramanian, R.S.; Balasubramaniam, R. The Motion of Bubbles and Drops in Reduced Gravity, Cambridge University Press. 2001.

[6] Barton, K.D.; Subramanian, R.S. Thermocapillary migration of a liquid drop normal to a plane surface, J. Colloid Interface Sci. 1990, 137 (1), 170–182.

[7] Chen, S.H.; Keh, H.J. Thermocapillary motion of a fluid droplet normal to a plane surface, J. Colloid Interface Sci. 1990, 137 (2), 550–562.

[8] Chen, J.; Dagan, Z.; Maldarelli, C. The axisymmetric thermocapillary motion of a fluid particle in a tube, J. Fluid Mech. 1991, 233, 405–437.

[9] Keh, H.J.; Chen, L.S. Droplet interactions in axisymmetric thermocapillary motion, J. Colloid Interface Sci. 1992, 151 (1), 1–16.

[10] Keh, H.J.; Chen, P.Y.; Chen, L.S. Thermocapillary motion of a fluid droplet parallel to two plane walls, Int. J. Multiph. Flow. 2002, 28 (7), 1149–1175.

[11] Nas, S.; Muradoglu, M.; Tryggvason, G. Pattern formation of drops in thermocapillary migration, Int. J. Heat Mass Transfer. 2006, 49 (13–14), 2265–2276.

[12] Yin, Z.; Chang, L.; Hu, W.; Gao, P. Thermocapillary migration and interaction of two nondeformable drops, Appl. Math. Mech. 2011, 32 (7), 811–824.

[13] Brady, P.T.; Herrmann, M.; Lopez, J.M. Confined thermocapillary motion of a three-dimensional deformable drop, Phys. Fluids. 2011, 23 (2), 022101-022111.

[14] Ahmed G. Salem; Faltas, M.S.; Sherief, H.H. The Stokes thermocapillary motion of a spherical droplet in the presence of an interface, European Journal of Mechanics / B Fluids. 2023, 101, 303–319.

[15] Chiu, H.C.; Keh, H.J. Thermocapillary migration of a fluid sphere in a circular tube, Am. J. Heat Mass Transf. 2016, 3 (1), 15–36.

[16] Faltas, M.S.; Sherief, H.H.; Allam A. Allam; Nashwan, M.G.; El-Sayed, M. Thermophoresis of a spherical particle in a permeable microchannel with thermal stress slip, Physical Review Fluids. 2023, 8, 054102.

[17] Chen, J.; Dagan, Z.; Maldarelli, C. The axisymmetric thermocapillary motion of a fluid particle in a tube. Journal of Fluid Mechanics. 1991, 233, 405-437.

[18] Mahesri, S.; Haj-Hariri, H.; Borhan, A. Effect of interface deformability on thermocapillary motion of a drop in a tube. Heat and Mass Transfer. 2014, 50, 363-372.

[19] Keh, H. J.; Chen, P.Y.; Chen, L. S. Thermocapillary motion of a fluid droplet parallel to two plane walls. International Journal of Multiphase Flow. 2002, 28, 1149-1175.

[20] O'Neill, M.E.; Bhatt, B.S. Slow motion of a solid sphere in the presence of a naturally permeable surface, Q. J. Mech. Appl. Math. 1991, 44, 91.

[21] Happel, J.; Brenner, H. Low Reynolds Number Hydrodynamics: With Special Applications to Particulate Media (Springer Science and Business Media, New York, 2012).

[22] Reed, L. D. Low Knudsen number photopheresis, J. Aerosol Sci. 1977, 8, 123.

[23] Chang, Y.C.; Keh, H.J. Thermophoresis at small but finite Péclet numbers, Aerosol Sci. Technol. 2018, 52,1028.

[24] Beavers, G. S.; Joseph, D.D. Boundary conditions at a naturally permeable wall, J. Fluid Mech. 1967, 30,197.

[25] Saffman, P. On the boundary condition at the surface of a porous medium, MIT Stud. Appl. Math. 1971, 50, 93.

[26] Huan Keh, J.; Na Y. Ho. Some solutions of the cell model for a suspension of droplets in thermocapillary motion, J. Chin. Inst. Chem. Engrs. 1998, 29(6), 453-466.